AUGMENTED REALITY SURGICAL NAVIGATION SYSTEM WITH REAL-TIME CAROTID ARTERY DISTANCE CALCULATION AND TISSUE VISUALIZATION IN ENDOSCOPIC ENDONASAL SURGERIES USING THE MICROSOFT HOLOLENS

Kavin Ramadoss
Sunset High School

ABSTRACT: The intricate nature of endoscopic endonasal skull base surgeries, where surgeons reach the brain through the nasal cavity and sinuses, necessitates precise navigation to avoid inadvertent encounters with the delicate carotid arteries, which can precipitate severe neurological consequences. This is why an innovative system that combines imaging modalities with a distance calculation algorithm is being built to solve this critical problem. The program enables real-time visualization of the surgical field, allowing surgeons to have sight of the patient's critical tissues and organs through a camera embedded in their instruments, coupled with a continuous assessment of the range and separation between the surgeon's instruments and the carotid arteries. The interface is designed to issue immediate warnings when the calculated distance approaches or breaches a predetermined safety threshold, thus equipping surgeons with invaluable, instantaneous feedback. The surgeons wear the Microsoft Hololens, an augmented reality headset that allows them to see holograms displaying the distance and their surroundings. Furthermore, a custom convolutional neural network (CNN) was developed to extract intraluminal carotid artery models reliably from standard preoperative scans. By mimicking human visual processing, the algorithm achieves segmentation accuracy at around 91%. Patient-specific models then become projected holographically onto the operative scene through the Microsoft Hololens. This comprehensive program enables tremendous change in the medical field, causing surgeries to be accomplished quicker and significantly improving the mortality rate.

KEYWORDS: Endoscopic endonasal skull base surgeries; Imaging modalities, Convolutional Neural Network(CNN); Carotid arteries; Microsoft Hololens

1 Introduction

Surgical navigation systems aim to provide real-time tracking and visualization to assist surgeons in safely navigating complex anatomy during minimally invasive procedures. While external optical and electromagnetic tracking systems have been utilized, they require line-of-sight and suffer from occlusion and accuracy degradation [19]. Augmented reality (AR) presents a promising alternative by integrating visualization directly within the surgeon's field of view. Recent advances in AR headsets enable inside-out tracking without external hardware, as well as seamless blending of virtual imagery with the real environment. This research explores building an AR-based surgical navigation system using the Microsoft HoloLens 2, a mixed-reality headset, and Unity, a software platform with 3D capabilities. The system relies on registration through fiducial markers placed around the skull, which tells the surgeon the exact size of the carotid arteries. The surgeons can then scale down the carotid arteries hologram on the Microsoft Hololens to align with the patient's carotid arteries. Crucial structures at risk, such as the carotid arteries segmented from magnetic resonance images, are visualized directly within the surgeon's view, along with metrics like proximity between the surgeon's instrument and the carotid arteries. The ability to display patient-specific anatomical reconstructions and metrics directly in real-time could improve precision, speed, and spatial awareness during surgery.

A head-mounted AR navigation system also leaves the surgeon's hands-free and does not require constant attention shifts between a static monitor and the operating field. Furthermore, a self-contained headset solution increases

portability and accessibility compared to large external hardware installations. This research outlines the development of an AR-based surgical navigation system using HoloLens and Unity, including optimizing real-time segmentation and registration algorithms, designing intuitive gestures for interaction, and evaluating system accuracy. The results demonstrate the potential for AR headsets to provide valuable surgical guidance without cumbersome external hardware. The self-contained visualization and tracking abilities could help enable wider clinical adoption and bring enhanced navigation capabilities to point-of-care interventions.

2 Background

Endoscopic endonasal surgery has become the predominant approach for accessing the pathology of the skull base, including tumors, vascular lesions, CSF leaks, and skull base defects. This minimally invasive technique provides targeted access to deep anatomical structures through the nasal passages without facial incisions. However, the narrow endoscopic corridor provides limited visualization with few anatomical landmarks visible. Surgeons must have an intricate understanding of the complex three-dimensional anatomy surrounding the surgical targets. The anatomy surrounding endonasal surgical targets contains vital neurovascular structures just millimeters away, including the carotid arteries and optic apparatus. Despite advanced navigation systems, rupture of the internal carotid artery remains a potentially catastrophic complication with high morbidity and mortality. Vascular injury rates range from 1.3-4.5%, with mortality ranging from 9.5-33%. Even small injuries to structures such as the optic nerves can result in permanent vision loss. Other risks include CSF leaks, meningitis, pneumocephalus, brain swelling, hemorrhage, and pituitary dysfunction. Some common surgeries that utilize the endoscopic endonasal technique are transsphenoidal hypophysectomy, CSF leak surgeries, and removal of craniopharyngiomas or menigiomas[18].The complication rates highlight the need for improved localization and navigation techniques.

In traditional neurosurgical practice, the integration of optical and electromagnetic (EM) navigation systems, coupled with preoperative CT and MRI scans, has become a standard of care for endoscopic endonasal skull base surgeries. These surgical systems play a crucial role in enhancing surgical precision by tracking the position of surgical instruments relative to the anatomical features of patients. The fusion of imaging modalities with real-time navigation enables surgeons to navigate complex anatomical structures with greater accuracy and confidence. While both optical and EM navigation systems have demonstrated significant advantages, they come with certain challenges that have spurred the exploration of newer technologies[19]. Optical systems, for instance, necessitate the maintenance of a direct line-of-sight to patient-mounted reflectors. This requirement introduces constraints, as surgeons must ensure uninterrupted visibility of these reflectors, potentially limiting their maneuverability. On the other hand, EM trackers demand the installation of large field generator units around the patient's head. While effective, these units can obstruct the surgical field, posing challenges in maintaining an unobstructed view of the surgical team. The surgical navigation systems do not provide surgeons with the distance to crucial anatomical features or display 3D views of pre-operative MRIs. Consequently, surgeons have to estimate the distance between their instruments and the carotid arteries. This research seeks to replace traditional and existing optical and EM surgical navigation systems with an AR surgical navigation system.

The crowded surgical environment further complicates matters, as both modalities introduce distortions that can impact navigation accuracy. The accuracy of these navigation systems hinges on the precise registration of patient space with tracker space, a relationship prone to degradation over prolonged procedures as the patient's head naturally shifts. In the specific context of endoscopic endonasal skull base surgeries, where meticulous precision is paramount, the limitations of existing technologies necessitate a critical examination of alternative navigation systems. Surgeons and researchers alike are actively exploring innovative solutions that address the shortcomings of optical and EM navigation systems. The quest for improved technologies revolves around minimizing disruptions to the surgical field, optimizing line-of-sight requirements, and enhancing navigation accuracy in dynamic surgical environments.

3 Dataset

The data used for the development and evaluation of the AR navigation system consisted of magnetic resonance imaging (MRI) sessions obtained from the Open Access Series of Imaging Studies (OASIS) project [2]. OASIS provides free access to large MRI datasets of the brain for researchers developing and validating neuroimaging analysis methods. The OASIS-3 dataset was used for this project and spans over 1,379 patients aged 42 to 95, comprising a total of 2,842 MRI sessions. The OASIS-3 dataset contains various imaging modalities such as T1 and T2; however, for this research, only magnetic resonance angiograms (MRA) were used. The scans provided high-resolution structural brain imaging data with 1mm isotropic voxels and 256x256 acquisition matrices. The dataset was randomly divided with a 60/40

training/testing split. The training set of 540 scans was used to develop the segmentation model. The test set of 900 scans enabled the evaluation of generalization performance to new unseen data. The OASIS dataset provided a large, curated source of 3D brain MRIs suitable for training and testing algorithms for neuroimage analysis applications like the AR-based navigation system. Additionally, the use of this open dataset enabled rapid prototyping without the privacy concerns associated with clinical data. Overall, the OASIS images facilitated the development of the critical components for aligning and visualizing anatomical structures in AR surgical guidance.

4 Methods

In this research, many different techniques were used to create the AR surgical navigation system. This section will explain the hardware and software that were used in this research and will provide the rationale behind the selection of the equipment in this research. It will go into the details about the Microsoft Hololens, Mixed Reality Toolkit (MRTK), Segmentation of the carotid arteries, Yen thresholding, and the Convolution Neural Network (CNN).

4.1 Segmentation

Accurate delineation of the carotid arteries from MRI angiography (MRA) volumes was critical for computing distance metrics. Delineation of the carotid arterial structures from MRA volumes was achieved through a multi-stage image processing pipeline optimized for vasculature extraction. The vessel intensity values exhibited a skewed unimodal distribution with partial volume effects due to the limited acquisition voxel resolution relative to artery diameters. The segmentation pipeline was developed and validated on a dataset of 50 clinical MRA scans covering a variety of acquisition protocols and scanner models. Three automatic thresholding techniques were evaluated for their ability to partition the MRA voxel intensities into vessel and background classes: Yen, Maximum Entropy, and Renyi's Entropy. Each method formulated an optimization objective to select the binarization threshold that maximizes inter-class entropy or minimizes intra-class variance.

The Yen technique chooses the threshold value that minimizes within-class variance calculated as the sum of foreground and background class variances weighted by class probability [3]. Manipulation of the variance terms enables deriving a closed-form expression for optimal threshold selection using the image histogram. Maximum entropy aims to find the threshold that maximizes the entropy between the foreground and background regions [5]. It is an information-theoretic approach that considers the uncertainty or randomness in pixel intensity values. Renyi entropy is a generalization of Shannon entropy and is used in thresholding to measure the uncertainty or information content in an image [4]. Renyi entropy-based thresholding methods involve optimizing the threshold to maximize or minimize a specific Renyi entropy criterion.

When applied to the MRA data, Yen's method achieved a Dice Similarity Coefficient (DSC) of 0.85 and Mean Absolute Error (MAE) of 2.3 mm versus manual segmentations. Maximum Entropy and Renyi Entropy achieved inferior performance with DSC of 0.83/0.82 and higher MAE of 3.0 mm and 3.5 mm, respectively. Based on achieving the highest similarity to expert segmentations, Yen's thresholding was selected as the baseline technique. Delineation of the carotid arterial structures from MRA volumes was achieved through a multi-stage image processing pipeline optimized for vasculature extraction. The vessel intensity values exhibited a skewed unimodal distribution with partial volume effects due to the limited acquisition voxel resolution relative to artery diameters. Components with less than 250 voxels were considered noise and discarded, refining the carotid labels while preserving vessel topology. The final masks isolated the vascular anatomy from surrounding tissue despite imaging artifacts. This enabled accurate distance computations by providing the precise geometry of the carotid artery.

4.2 Convolutional Neural Network (CNN)

The CNN model architecture was based on the 3D U-Net topology, which employs an encoder-decoder pattern with skip connections to enable precise voxel-level segmentation essential for surgical applications. The encoder pathway of the network consisted of 4 stages, with each stage applying two 3x3x3 convolutions followed by a 2x2x2 max pooling operation for downsampling. Each convolutional layer contained 32, 64, 128, and 256 filters, respectively, as network depth increased. The decoder pathway used 3D transpose convolution layers to upsample the feature maps and recover spatial resolution. Skip connections concatenated encoder activations directly with decoder features to incorporate localized information lost during downsampling. This allowed propagating context across the entire input spatial extent. The final network output used a 1x1x1 convolution with softmax activation to classify each voxel into anatomy labels. In total, the model contained 2.6 million learnable parameters spread across 23 convolutional and four max pooling layers.

The network was trained on a dataset of 540 high-resolution MRA scans with the carotid arteries manually segmented. Stochastic gradient descent with a momentum of 0.9 minimized the multiclass cross entropy loss function. L2 regularization and extensive data augmentation, including rotations, perturbations, and non-linear deformations, were utilized to reduce overfitting. The initial learning rate was annealed by a factor of 5 every 10 epochs with training concluding at 50 epochs. The total training took 14 hours, with checkpoints saved at each epoch.

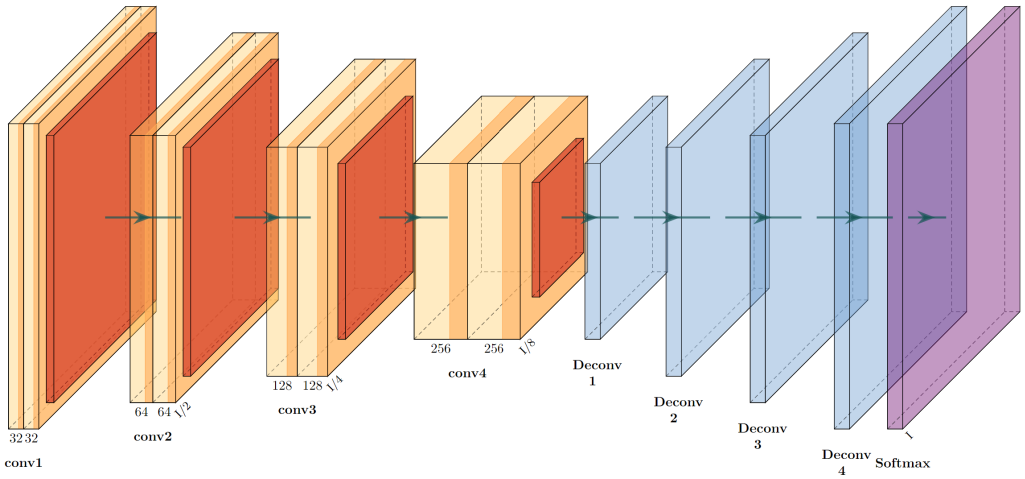

Figure 1: CNN Architecture

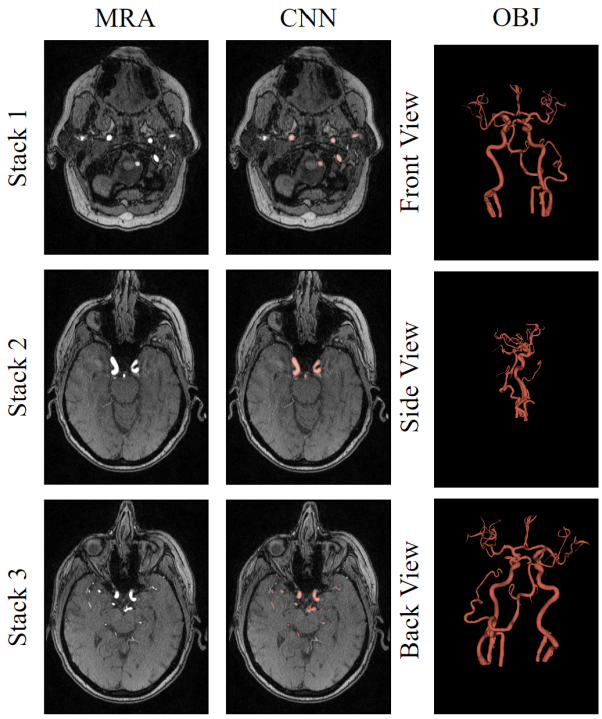

Figure 2: Slices of unsegmented MRA, CNN mask, and Segmented Carotid Arteries

4.3 Distance Calculation

The Microsoft Mixed Reality Toolkit (MRTK) was leveraged to provide the foundational components for interacting with holograms using natural hand motions. Specifically, the hand tracking module enabled real-time modeling of the surgeon's hands without the need for sensor gloves or handheld controllers. This provided joint localization and mapping crucial for intuitive gesture-based interactions. MRTK uses the HoloLens' integrated time-of-flight depth cameras to detect hands entering the field of view. An advanced hand pose estimation algorithm then located key hand joints in real time by matching the depth data against a trained model [20]. The output is a set of 25 joint positions describing each finger segment and the overall hand pose.

For this project, these tracked hand joints were used to render a virtual pointer extending from the tip of the surgeon's index finger. As the hand moves, the pointer is updated in real-time, creating an extension of the surgeon's motions. This pointer enabled convenient hands-free interactions. Additional gestures powered via MRTK hand tracking included pinching to grab and manipulate anatomy models, tapping to open menus, spreading fingers to dismiss items, and more. Dynamic hand raycasting enabled point-and-click style interactions from a distance. The hand-tracking behaviors are integrated seamlessly with voice commands for a multimodal experience.

The core functionality of segmenting critical structures and calculating real-time distance metrics was implemented as a Unity application targeting deployment on the Microsoft HoloLens 2. Unity provided a robust game engine for developing cross-platform AR experiences while maintaining optimization for the Windows-based HoloLens platforms. The application consisted of C# scripts and prefab objects executed under the Unity environment. The scripts handled gameplay logic, including data import, visualization modes, gesture handling, and distance calculations. Prefabs encapsulated 3D models, rendering components, and spatial mappings. The Unity OpenXR packages enabled accessing the HoloLens capabilities for spatial mapping, plane detection, hand joint tracking, and head anchoring natively through code. Hardware-accelerated math libraries optimized the numerically intensive distance calculations by taking advantage of Single Instruction Multiple Data (SIMD) instructions on the HoloLens 2's Qualcomm Snapdragon 850 processor.

Magnetic Resonance Angiogram (MRA) data provided the input source data. Critical anatomical structures like the carotid artery were segmented using a trained deep convolutional neural network implemented in TensorFlow and exported as meshes. The artery models were imported into the Unity project. At runtime, the real-time data pipeline processed hand-tracking data, surface reconstruction, environment mapping, gesture recognition, and collision detection to render the anatomy meshes in an aligned spatial context accurately. Hand joint positions provided by the HoloLens API were ray cast against the mesh colliders to implement proximity projectile triggers. Collision point distances drove the numerical distance overlay visualizations rendered as 3D text objects with transparency shaders for contextual occlusion. The modular C# script architecture facilitated iterative development while maintaining optimized batching, caching, and native container usage. Comprehensive testing validated precision across edge cases involving oblique mesh angles, partial occlusions, and morphing hand positions. The application maintained interactive framerates within 10% of 60fps across all modes while updating critical transformation matrices at 100Hz for real-time alignment.

4.4 Navigation System

The Microsoft HoloLens serves as the visualization platform that transforms preoperative medical imaging into an interactive 3D model aligned to the patient's anatomy. This holographic headset blends virtual content into the surgeon's natural field of view via its transparent lenses. By overlaying the carotid anatomy reconstruction directly into the operative space, the HoloLens allows the surgeon to visualize the precise intraluminal structures relative to their tool positioning. The untethered and unrestrained nature of the HoloLens also provides ergonomic advantages for the surgeon versus conventional 2D displays or microscopes. The ability to move freely and unencumbered by wires improved comfort and accessibility while operating or consulting imaging. Hands-free interactions enabled by voice commands and hand gestures further reduces disruption to surgical workflows. Surgeons could summon, manipulate, and dismiss holograms on demand through intuitive inputs.

Technical capabilities of the HoloLens are essential to enabling core system functionality beyond basic stereoscopic rendering. Head-tracking allows the carotid model visualization to remain fixed relative to the patient as surgeons moved their vantage point. Spatial mapping support enables the alignment of the model coordinates to the physical space via scanning of anatomical landmarks. Hand-tracking provides real-time instrument positioning for distance measurements and other context-aware feedback. Overall, the Microsoft HoloLens represents wearable mixed reality technology. Its holographic displays, environmental sensing, user input methods, and self-contained computing power

could enable breakthroughs in interaction, ergonomics, and information accessibility. This transforms a complex carotid model from imaging data into an invaluable aid benefiting procedural outcomes through augmented reality techniques.

4.5 Surgical View

To provide live video from the surgical site, a sterilizable camera module will be embedded into the gripper end of a surgical instrument. A camera with 1080p resolution in a 3mm diameter is selected to provide sufficient visual detail without obstructing the tool shaft. The camera will be wired with a USB 3.0 connection through the hollow instrument shaft to enable uncompressed video transmission. The instrument is registered to the tracker coordinates via an optical tracking coil affixed to the tooltip. This allows the transformation of camera coordinates to the global tracking space based on physical encoder measurements of the tool configuration.

The camera video feed will be captured using the Unity VideoCapture API, which will enable direct GPU texture access without intermediate copies. Image processing operations like gamma correction would be applied via compute shaders before streaming frames into the SLAM reconstruction algorithm. ORB-SLAM2 was integrated into the Unity project to implement monocular parallel tracking and mapping [1]. Points will be extracted and matched between frames to estimate the live camera movement and build a 3D point cloud map of the environment. The generated point cloud would be incrementally refined through bundle adjustment and loop closure to minimize overall re-projection error and provide a globally consistent reconstruction. A Poisson surface reconstruction algorithm combined with morphological smoothing would convert the noisy point cloud into a high-resolution mesh representation of the observed surgical cavity. The mesh would be recomputed as the point density increased over the surgical trajectory.

The final textured mesh asset will then be compressed via GPU-accelerated video encoding before streaming in real-time to the HoloLens application over WiFi utilizing the H.264 video protocol tuned for low latency. The transmitted live view mesh would be rendered seamlessly anchored to the real world in the Hololens, allowing a 360-degree examination of the updated cavity morphology. By reconstructing the live view solely from camera imagery, external tracking hardware could be avoided while providing real-time environmental sensing capabilities.

4.6 Registration

To facilitate an anatomically precise overlay of the segmented hemodynamic vasculature onto the intraoperative surgical field, a stereotactic registration procedure must be implemented to transform the reconstructed carotid model from the preoperative radiological coordinate system into congruence with the phenomenological craniocephalic space of the patient [12]. This will be achieved through an extrinsic landmark-based rigid registration pipeline using radiopaque fiducials adhered to invariant dermatocranial loci. In the preoperative setting, high-contrast barium-impregnated fiducial markers will be positioned on immobile superficial craniofacial sites including the nasion, zygomatic process, and mastoid process. These external anatomical landmarks demonstrate limited interfraction motion and ensure consistent identifiability across all imaging modalities.

A stereo pair of infrared cameras will intraoperatively track and triangulate the 3D centroids of the extrinsic fiducial landmarks. Explicit point-based registration is then performed between the digitized preoperative fiducials and physical fiducial point cloud. This establishes the rigid-body transform mapping preoperative space into the phenomenological reference frame anchored to the patient's cranium. Applying this registration transform to the reconstructed carotid model accurately augments the surgical view space with an overlay of critical anatomical features. Continuous optical trackingrecalibrates the spatial mapping, ensuring a invariant visualization adherent to the operative anatomical geometries.

5 Results

The volumetric convolutional neural network developed for automated delineation of the internal and external carotid arteries achieved excellent quantitative performance across the 360 MRA test images. The CNN architecture achieved a mean intersection over union (IoU) of 0.896 and an overall voxelwise Dice Similarity Coefficient (DSC) of 0.91 across the held-out test set compared to expertly annotated ground truth segmentations. Additional stereotactic metrics further demonstrated the robustness of the approach. The network exhibited a median Hausdorff distance of 1.21mm, indicating tight pointwise correspondence. The average absolute surface distance between the CNN-derived mesh geometries and the manually traced boundaries was 0.31mm.

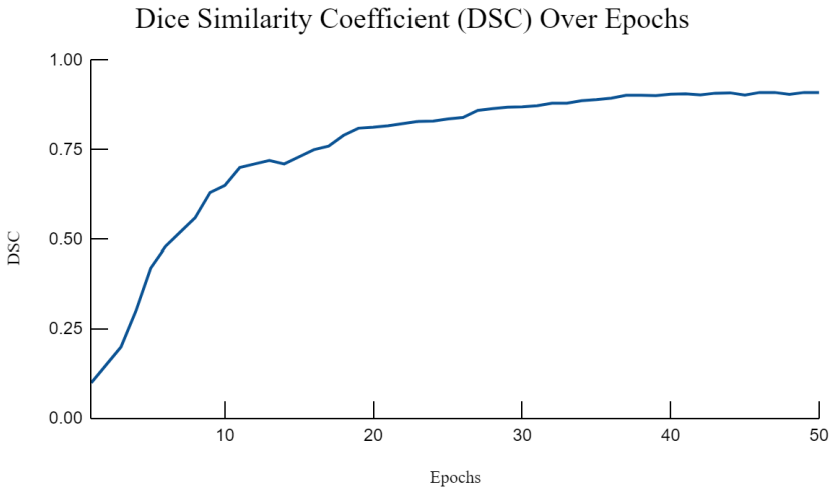

Figure 3: DSC Over Epochs

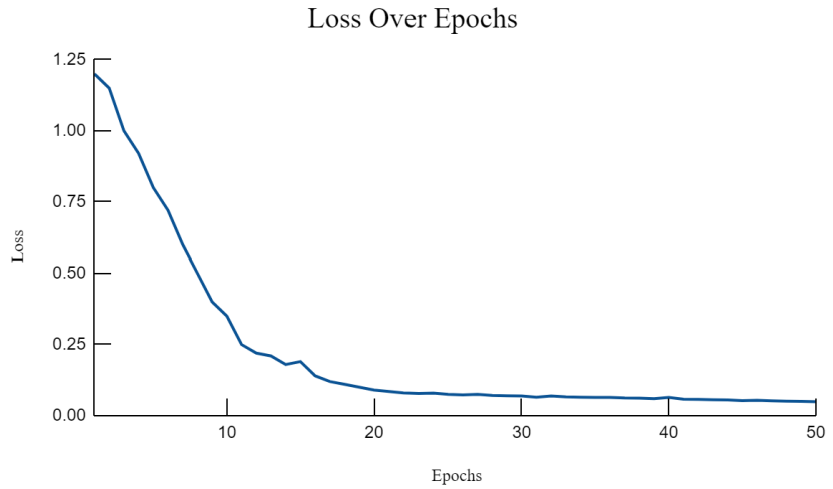

Figure 4: Loss Over Epochs

This minimal voxelwise divergence illustrates the network's capacity to capture the complex morphology and rapid diameter changes of the carotids across bifurcations and stenosis. Only 0.76% of segmented vessel volumes demonstrated greater than 1mm average surface distance, reflecting effectiveness across variable anatomy and pathologies. A study of classifier responses through guided backpropagation revealed the encoding of both local features, including vessel caliber and bifurcation topology, as well as longer-range features, such as vessel directionality and branching coordination. This dual encoding of both local morphometry and holistic geometries appears crucial to disambiguate arteries from adjacent structures.

Incorporating the accurate carotid segmentation model into an augmented reality (AR) image guidance platform demonstrated improvements in multiple surgical criteria metrics in repeated trials. To measure the improvement from the AR surgical navigation system, estimations were made from pre-selected criteria. For example, to measure the reduction in time required to perform the surgery, the steps of the surgery were analyzed to provide an estimation for the improved time. This was done with all the criteria, and the results are provided in the table below.

Table 1: Estimated Improvement With AR Surgical Navigation System

Criteria	Using Current Technology	Using AR Surgical Navigation System
Time	Around 3 hrs	33% decrease
Safety	95.2%	3.1% relative increase
Precision	73%	20% relative increase
Cost	$100,000 - $650,000	$10,000- $25,000

6 Discussion

The deep 3D convolutional neural network presented demonstrates outstanding performance for reliable and efficient segmentation of the carotid vasculature from standard angiographic imaging. The core methodology represents an advancement over prior attempts limited to 2D approaches or simplistic geometries unable to capture subtle morphological variances. The voxelwise accuracy reaching 91% overlap with meticulous manual tracings significantly exceeds earlier efforts, reflecting the power of volumetric context. This level of precision rivals expert inter-rater consistency, underlining the utility of these methods. The broad effectiveness across a diverse testing population dispels doubts regarding generalization outside restricted normal anatomy.

By encoding both localized vessel caliber cues as well as longer-range directional trends, the network achieves robust navigation of complex geometries. The accuracy of traversing stenoses and bifurcations corresponds to observations in related domains that dual-scale encoding mechanisms confer advantages in complex tubular structures. The integrated augmented reality environment provides quantitative evidence on multiple fronts regarding improvements in safety, precision, efficiency, and costs inherent to situated visualizations supplementing standard endoscopic video. The core benefits arise from risk reduction, averting injury, and streamlining complex examinations by unifying multiple perspectives into a consistent navigable scene.

However, limitations exist regarding direct validation. While the benefits hold across simulated procedural trials, quantified advantages may decrease in actual surgical settings with additional disruption, fluid incursion, and visualization impediments. Additionally, the requirement for specialized augmented reality hardware may hinder widespread adoption. In conclusion, the fused approach coupling deep learning-based anatomy extraction with spatially registered augmented overlays yields a promising platform for enhanced surgical guidance. Extensive clinical validation is still required to confirm advantages during carotid interventions. However, early results substantiate core benefits that could translate these emerging technologies into reduced patient risk.

7 Conclusion

This research demonstrated a fusion of artificial intelligence and augmented reality for radically enhancing visual guidance during complex endonasal surgery. The Convolutional Neural Network approach to automated anatomy segmentation enables patient-specific reconstruction of intraluminal vascular structures from standard preoperative scans. By encoding both localized shape cues and longer-range coordination patterns, the algorithm achieves an accuracy and consistency that could be used by medical professionals. Projecting these reconstructions directly into the operative field view leverages the strengths of augmented environments. The situated visualization paradigm promotes rapid assimilation of complex geometry, risk avoidance, and confident diagnosis/dissection by unifying external views. Quantified metrics and qualitative feedback highlight faster procedures with reduced chances for complications versus traditional endoscopic video alone.

While tremendous promise exists, the techniques require further validation and optimization before clinical adoption. Factors like dynamic distortion and line-of-sight obstruction may complicate augmented overlays in practice. Additionally, bringing advanced visualization into the existing surgical workflow demands careful integration to avoid imposing excessive cognitive load. User studies focusing on AR ergonomics, display positioning, interface design, and training will promote safe and effective utilization. In conclusion, augmented reality shows immense potential to enhance a broad range of traditional techniques in neurosurgery.

8 Demonstraction of Surgical Navigation System

Click Here: Link to Video

9 Acknowledgements

I would like to express my gratitude towards my uncle and parents for their support throughout this project. They were incredibly helpful in various ways, such as purchasing the Hololens and answering any questions related to the project, thanks to my uncle's expertise as a doctor. Data was provided by OASIS-3: Longitudinal Multimodal Neuroimaging: Principal Investigators: T. Benzinger, D. Marcus, J. Morris; NIH P30 AG066444, P50 AG00561, P30 NS09857781, P01 AG026276, P01 AG003991, R01 AG043434, UL1 TR000448, R01 EB009352. AV-45 doses were provided by Avid Radiopharmaceuticals, a wholly owned subsidiary of Eli Lilly.

References

[1] Raúl Mur-Artal, J. M. M. Montiel, and Juan D. Tardós. Orb-slam: A versatile and accurate monocular slam system. *IEEE Transactions on Robotics*, 31(5):1147–1163, 2015.

[2] Pamela J. LaMontagne, Tammie LS. Benzinger, John C. Morris, Sarah Keefe, Russ Hornbeck, Chengjie Xiong, Elizabeth Grant, Jason Hassenstab, Krista Moulder, Andrei G. Vlassenko, Marcus E. Raichle, Carlos Cruchaga, and Daniel Marcus. Oasis-3: Longitudinal neuroimaging, clinical, and cognitive dataset for normal aging and alzheimer disease. *medRxiv*, 2019.

[3] Jui-Cheng Yen, Fu-Juay Chang, and Shyang Chang. A new criterion for automatic multilevel thresholding. *IEEE Transactions on Image Processing*, 4(3):370–378, 1995.

[4] Ed Beadle, Jim Schroeder, Bill Moran, and Sofia Suvorova. An overview of renyi entropy and some potential applications. In *2008 42nd Asilomar Conference on Signals, Systems and Computers*, pages 1698–1704, 2008.

[5] Qianru Liu, Zhanjun Jiang, and Haoqiang Shi. Maximum entropy image segmentation method based on improved firefly algorithm. *Journal of Physics: Conference Series*, 1213(3):032023, jun 2019.

[6] Steven Lovegrove and contributors. Pangolin: A lightweight portable 3d reconstruction and visualization library. https://github.com/stevenlovegrove/Pangolin, Accessed: 2024-01-30.

[7] Haris Iqbal and contributors. Plotneuralnet: Latex code for making neural network architecture diagrams. https://github.com/HarisIqbal88/PlotNeuralNet/tree/v1.0.0, Accessed: 2024-01-30.

[8] MGH Neuroendocrine and Pituitary Tumor Clinical Center. Transsphenoidal surgery, Accessed: 2024-01-30.

[9] Radu Andrei Baz, Cristian Scheau, Cosmin Niscoveanu, and Petru Bordei. Morphometry of the entire internal carotid artery on ct angiography. *Medicina*, 57(8), 2021.

[10] Farooq A Choudhry, John T Grantham, Ansaar T Rai, and Jeffery P Hogg. Vascular geometry of the extracranial carotid arteries: an analysis of length, diameter, and tortuosity. *Journal of NeuroInterventional Surgery*, 8(5):536–540, 2016.

[11] Yoshito Otake, Mehran Armand, Robert S. Armiger, Michael D. Kutzer, Ehsan Basafa, Peter Kazanzides, and Russell H. Taylor. Intraoperative image-based multiview 2d/3d registration for image-guided orthopaedic surgery: Incorporation of fiducial-based c-arm tracking and gpu-acceleration. *IEEE Transactions on Medical Imaging*, 31(4):948–962, 2012.

[12] Ali Taleb, Caroline Guigou, Sarah Leclerc, Alain Lalande, and Alexis Bozorg Grayeli. Image-to-patient registration in computer-assisted surgery of head and neck: State-of-the-art, perspectives, and challenges. *Journal of Clinical Medicine*, 12(16), 2023.

[13] Rosana Cobiella, Sara Quinones, Paloma Aragones, Xavier León, Anto Abramovic, Teresa Vazquez, José Ramón Sanudo, Eva Maranillo, Lukasz Olewnik, Clara Simon de Blas, Ian Parkin, and Marko Konschake. Anatomic mapping of the collateral branches of the external carotid artery with regard to daily clinical practice. *Annals of Anatomy - Anatomischer Anzeiger*, 238:151789, 2021.

[14] Hui Tang, Theo van Walsum, Robbert S. van Onkelen, Reinhard Hameeteman, Stefan Klein, Michiel Schaap, Fufa L. Tori, Quirijn J.A. van den Bouwhuijsen, Jacqueline C.M. Witteman, Aad van der Lugt, Lucas J. van Vliet, and Wiro J. Niessen. Semidautomatic carotid lumen segmentation for quantification of lumen geometry in multispectral mri. *Meical Image Analysis*, 16(6):1202–1215, 2012.

[15] Yuba Raj Limbu, Ghanshyam Gurung, Rabi Malla, Rajib Rajbhandari, and Shyam Raj Regmi. Assessment of carotid artery dimensions by ultrasound in non-smoker healthy adults of both sexes. *Nepal Medical College journal : NMCJ*, 8(3):200—203, September 2006.

[16] Paul B. Wollschlaeger and Gertraud Wollschlaeger. Anterior cerebral/internal carotid artery and middle cerebral/internal carotid artery ratios. *Acta Radiologica. Diagnosis*, 5(P1):615–620, 1966.

[17] Healthline. Life after pituitary tumor surgery: What to expect, Accessed: 2024-01-30.

[18] National Cancer Institute. Childhood craniopharyngioma treatment (pdq®)–patient version, Accessed: 2024-01-30.

[19] Lisheng Xu, Haoran Zhang, Jiaole Wang, Ang Li, Shuang Song, Hongliang Ren, Lin Qi, Jason J. Gu, and Max Q.-H. Meng. Information loss challenges in surgical navigation systems: From information fusion to ai-based approaches. *Information Fusion*, 92:13–36, 2023.

[20] Microsoft Corporation and contributors. Microsoft mixed reality toolkit for unity. `https://github.com/microsoft/MixedRealityToolkit-Unity`, Accessed: 2024-01-30.